The theoretical approach of how to predict the critical rotational speed of the rotating nozzle in flashing purification to increase the evaporation rate

by Hery Sonawan -

Submission date: 21-Jun-2023 11:25AM (UTC+0700)
Submission ID: 2120117754
File name: le_in_flashing_purification_to_increase_the_evaporation_rate.pdf (730.79K)
Word count: 4764
Character count: 23315

The theoretical approach of how to predict the critical rotational speed of the rotating nozzle in flashing purification to increase the evaporation rate

The theoretical approach of how to predict the critical rotational speed of the rotating nozzle in flashing purification to increase the evaporation rate

Hery Sonawan[1], Abdurrachim Halim[2], Nathanael P. Tandian[3]

[1,2] Program Studi Teknik Mesin, Universitas Pasundan, Jalan Setiabudi no. 193
[3] Fakultas Teknik Mesin dan Dirgantara, Institut Teknologi Bandung

Abstract. We developed a new flashing method in this study to improve the evaporation rate in flashing purification. In this case, a stationary nozzle is replaced by a rotating nozzle during the flashing process. The use of a rotating nozzle may distribute water droplets in previously unreachable spaces; the more droplets, the greater the evaporation rate. The use of a rotating nozzle during flashing causes problems if the rotational speed causes the water droplets to collide. To avoid a collision, a rotating nozzle must rotate at an appropriate rate. The kinematics of drifting water droplets after being sprayed by a rotating nozzle can be used to calculate this speed. It could be calculated by periodically observing droplet movement to determine the critical rotational speed of a rotating nozzle. By studying the trajectories of water droplet movement after being sprayed by a rotating nozzle, we can obtain no droplet collision circumstances. Water droplet evaporation during drifting reduces droplet size, resulting in a lower nozzle rotational speed to avoid a collision. For a water particle diameter of 153.5 μm, the smallest nozzle rotational speed predicted is 85.4 rpm. A droplet with a diameter of 80 μm produces 82 rpm of nozzle rotational speed, while a droplet with a diameter of 40 μm produces 80 rpm of nozzle rotational speed. Evaporation may reduce the size of the water droplets during the flashing process. To avoid droplet collision and increase evaporation rate, finer water droplets require a lower nozzle rotational speed.

1. Introduction

Recently, some flashing desalination technologies in multi-effect distillation have been operating with fixed nozzles. The use of stationary nozzles only distributes water droplets in one direction, leaving empty spaces within the chamber. The number of droplets sprayed by the nozzle determines the rate of evaporation in the chamber. The higher the evaporation rate, the more droplets there are.

By adding more fixed nozzles or by rotating the nozzles, it is possible to raise the number of droplets in the chamber. A rotating nozzle can disperse water droplets in areas where a stationary nozzle could not. As a result, the rotating nozzle multiplies the number of droplets in the chamber. In applying the rotating nozzle in the chamber, it must consider how fast the nozzle rotates.

If it is not appropriate, it may not result in an increase in evaporation rate. As a consequence, the nozzle rotational speed must be precisely controlled. We conducted research to determine the proper rotational speed. The estimated rotating speed of the nozzle may increase the number of droplets in the chamber. If the droplets do not collide, the number of droplets increases. If the given rotational speed causes the water droplets to collide with each other, using a rotating nozzle during flashing still leaves the problem. By studying the trajectories of water droplet movement after being sprayed by a rotating nozzle, we can obtain no droplet collision circumstances.

Kitamura et al., Miyatake et al., Mutair & Ikegami, Muthunayagam et al., El-Fiqi et al., and Goto et al. used stationary nozzles in their flashing experiments (1-6). A stationary nozzle flashes water or other fluids up and down in the vacuum chamber. Some droplets evaporate, while others collide to form larger droplets. Because there are several droplet trajectories that intersect at a point, the theorem of collisions between drifting water droplets is very strong.

Mutair and Ikegami conducted a study on improving the vapor evaporation desalination system by utilizing the heat of seawater (3). In his research, a nozzle pointed vertically upward does the water spraying. The variables investigated were superheated degree and spray speed. The initial feed-water temperature can increase the evaporation rate. Their study produced an empirical equation that can predict the spray distance, leading to water evaporation. This equation is useful for the design of the evaporation chamber.

A vapor evaporation technique that runs at vacuum pressure was developed as a research result by Muthunayagam et al. (4). A pilot plant demonstrated the feasibility of the desalination process using low-pressure seawater evaporation at temperatures ranging from 26 to 32 degrees Celsius. The system operates at a vacuum pressure of between 1.3 and 2.3 kPa. Using a swirl nozzle, seawater is sprayed into the vapor chamber as a fine droplet and evaporates at low pressure. Vapor condensation occurs within a shell and tube heat exchanger. Theoretically, fresh-water production reached 4% and water condensate quality is excellent. They test the performance of the pilot plant at various feed water temperatures, vacuum pressures, and water injection pressures.

Ikegami et al. conducted a comparison study of a spray flash desalination process using an upward and downward jet flash evaporation method (7). A series of experiments were conducted to investigate the effect of injection direction on the spray flash evaporation phenomenon. They used a tube-type nozzle with an internal diameter of 20.0 mm and a length of 81.3 mm in the experiment. El-Fiqi et al. also conducted research on flash evaporation (5). Flashing experiments were carried out at low pressure through a superheated jet nozzle in their study. The test employs a fixed nozzle with a diameter of less than 0.4 mm and an injection pressure of up to 6 bars, superheated degrees ranging from 2°K to 18°K, inlet feed temperatures ranging from 40 to 70 °C, and mass flow rate variations. Goto et al. also simulate a desalination system using spray flash (6).

Karami et al. investigated the flow-breaking process to reduce droplet size followed by evaporation (8). They conducted an experiment to determine how flashing influenced sprays from splash-plate nozzles. The investigation focused on the effect of injection temperature, pressure, and fluid transport system on the flow area inside the nozzle, the breakup mechanism, and the size of the water particles. The study discovers particle size and disintegration mechanisms, which are highly dependent on injection temperatures and low flow areas. At temperatures several degrees above the saturated temperature, flashing has been observed. Water particle fineness occurs over a narrow temperature range. Further temperature increases have no effect on particle size.

El-Zahaby et al. also attempted to increase condensate productivity through the use of flash evaporation (9). They put a solar desalination system with a flashing chamber through its paces. The study discovered that the system's productivity and performance were significantly positive depending on the pure water mass flow rate and linear velocity of the nozzle holders, and that the use of porous media in the sup as a heat storage medium increased productivity and performance slightly. Chen et al. investigated the flash evaporation phenomenon of a hot water jet sprayed with a fixed nozzle into a low-pressure chamber (10). Due to the flash atomization effect, the water jet shatters into droplets at low flow velocity.

2. Methodology

It could theoretically be calculated by periodically observing droplet movement to determine the critical rotational speed of a rotating nozzle. In the Cartesian coordinates, a point represents a water particle, as shown in Figure 1. The water particle movement is represented on each coordinate axis by velocity and its movement as a function of time Δt.

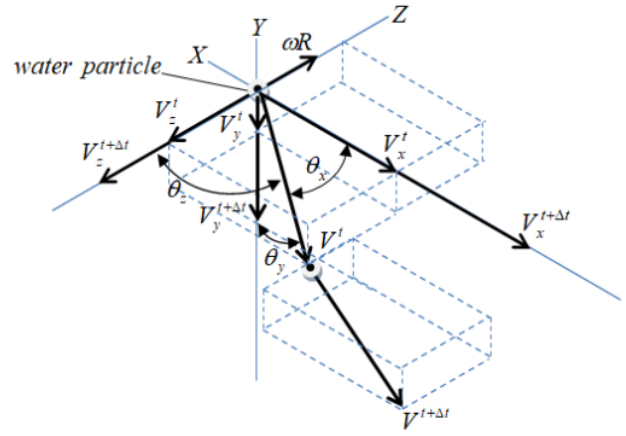

Figure 1. Kinematics of water droplet as a particle when spraying out of the nozzle

Droplets tend to collide as they move through the chamber. It took more than a droplet to analyze the collision between them. Five droplets were depicted in this study as five points in the plane of a nozzle hole, as shown in Figure 2. Each droplet's initial coordinates are defined by a pair of positions and angles. A specific spray corner can be found at the tip of a nozzle hole. Figure 2 depicts the angle of θ_x, θ_y, and θ_z as a representation of droplet location coordinates. Droplets drifted by, leaving different directions and trajectories behind the nozzle hole. A nozzle has a hole diameter of 0.3 mm and a maximum water flow of 5 l/h as a flow parameter in this study. The water velocity (V_{water}) ejected from the nozzle is shown in Equation (1).

$$V_{water} = \frac{\dot{V}}{A_N} = \frac{1.4 \cdot 10^{-6}\, m^3/s}{\frac{\pi}{4}(0.0003\, m)^2} = 19.65\, m/s \quad (1)$$

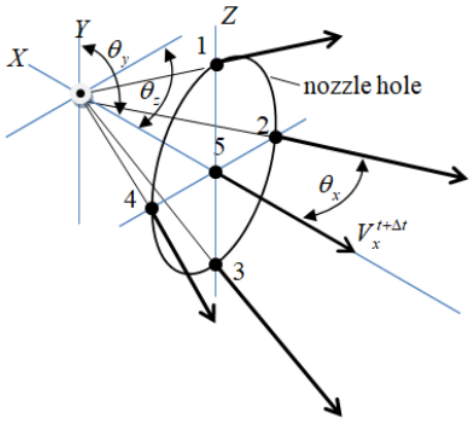

Figure 2. The coordinate system represents droplets' positions shortly after exiting the nozzle hole

After leaving the nozzle hole, each droplet has an initial velocity of 19.65 m/s. Droplet D5 (in Figure 2, D5 denotes the fifth droplet) is used as an example to analyze droplet movement from time to time. The droplet is represented by a tiny ball with d diameter and an initial velocity of 19.65 m/s, as calculated by Equation (2).

$$\mathrm{Re} = \frac{\rho_{air} \times V_{water} \times d}{\mu_{air}}$$
$$C_d = \left[\left(\frac{24}{\mathrm{Re}} \right)^{0.52} + 0.32^{0.52} \right]^{1/0.52} \quad (2)$$
$$F_d = C_d \frac{1}{2} \rho_{air} \left(\frac{\pi}{4} d^2 \right) V_{water}^2$$

The direction of viscous as a vector is opposite to the direction of droplet velocity. The velocity V_{water} and viscous F_d were represented in each axis by $V_x; V_y; V_z$ and $F_{d,x}; F_{d,y}; F_{d,z}$. While droplet #5 left the nozzle hole (at t = 0s), the initial coordinate was $\theta_x = 0^o; \theta_y = 90^o; \theta_z = 90^o$, and the velocity in the tangential direction (V_z) is known as ωR (R is the radial distance from the center of the rotor to the tip of the nozzle). Therefore, the velocity and viscous formulation at each axis are represented by Equation (3).

$$V^2 = V_x^2 + V_y^2 + V_z^2$$
$$V_x^t = V\cos\theta_x; \quad V_y^t = V\cos\theta_y; \quad V_z^t = V\cos\theta_z \quad (3)$$
$$F_{d,x}^t = F_d\cos\theta_x; \quad F_{d,y}^t = F_d\cos\theta_y; \quad F_{d,z}^t = F_d\cos\theta_z$$

Due to the viscous force, the droplets decelerated as written by Equation (4).

$$a_x^t = \frac{F_{d,x}^t}{m}; \quad a_y^t = \frac{F_g - F_{d,y}^t}{m}; \quad a_z^t = \frac{F_{d,z}^t}{m} \quad (4)$$

The deceleration is used to calculate droplet velocity in further time (t+Δt) along with the angle, as shown in Equation (5).

$$V_x^{t+\Delta t} = V_x^t - a_x^t \Delta t$$
$$V_y^{t+\Delta t} = V_y^t + a_y^t \Delta t$$
$$V_z^{t+\Delta t} = V_z^t - a_z^t \Delta t$$
$$\vec{V}^{t+\Delta t} = \vec{V}_x^{t+\Delta t} + \vec{V}_y^{t+\Delta t} + \vec{V}_z^{t+\Delta t} \quad (5)$$
$$\theta_x^{t+\Delta t} = \cos^{-1} \frac{V_x^{t+\Delta t}}{V^{t+\Delta t}}$$
$$\theta_y^{t+\Delta t} = \cos^{-1} \frac{V_y^{t+\Delta t}}{V^{t+\Delta t}}$$
$$\theta_z^{t+\Delta t} = \cos^{-1} \frac{V_z^{t+\Delta t}}{V^{t+\Delta t}}$$

The trajectories of the droplets were calculated by assuming that they did not evaporate while drifting (or that the droplet size remained constant) and that the droplet drifted up to the furthest radial distance of 38 cm according to the radius of the vacuum chamber. Droplet trajectories along the X and Y axes can be calculated using Equations (6) and (7).

$$S_x^{t+\Delta t} = S_x^t + V_x^t \times \Delta t \quad (6)$$
$$S_y^{t+\Delta t} = S_y^t + V_y^t \times \Delta t \quad (7)$$

3. Result and Discussion

The calculated droplet diameter was 153.5 µm for an initial velocity of 19.65 m/s, spray angle of 50°, water droplet density of 998 kg/m^3, air density of 1,22 kg/m^3, air viscosity of 18.10-6 Pa.s, and a calculated step size of 0.001 seconds, according to Stokes' law. Figure 3 depicts the sketched trajectory obtained by using the droplet trajectory calculation in Equations (6) and (7) for five droplets.

Because droplets ejected from a nozzle rubbed against the air and gradually drifted due to gravity, droplets with a high velocity generated high viscosity, which was greater than gravity and formed a straight-line path. Continuous friction with air slows its movement over time, until it only moves in a downward vertical direction at a constant velocity (or called a sedimentation velocity).

In Figure 3, the trajectory of droplets D4, D5, and D2 (D2, D4 and D5 denotes the second, fourth and fifth droplet in Figure 2) showed the greatest distance of droplets in the X-axis direction. The three droplets move horizontally by up to 0.35 m. The droplets are affected by gravity after passing through a range of 0.35 m. As a result, the droplet descended vertically until it reached the sedimentation velocity. The three droplets traveled a total distance of 0.38 m.

Droplet D1 is depicted as a droplet above droplet D5 that moves to follow the bullet motion at a 25° initial angle based on the half nozzle spray angle. Droplet D1 drifted up to 0.32 m and then gradually decreased until it reached the sedimentation velocity. Droplet D1 traveled 0.35 m in the radial direction.

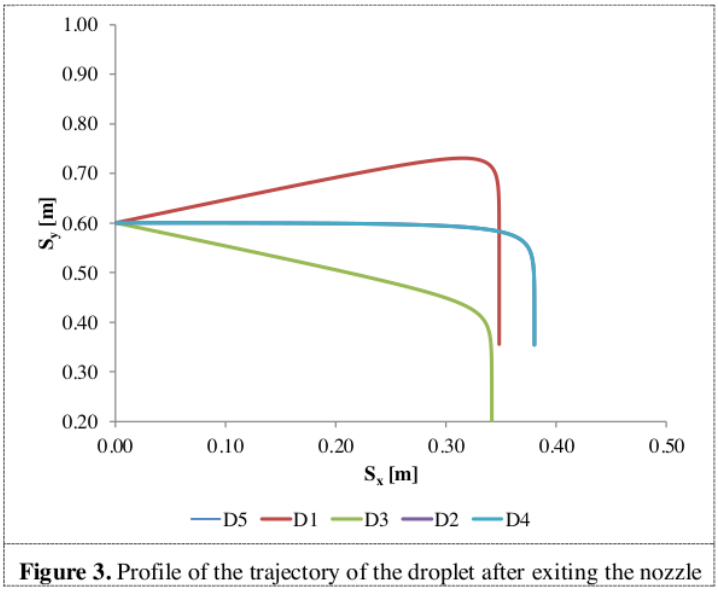

Figure 3. Profile of the trajectory of the droplet after exiting the nozzle

Droplet D3 had the shortest trajectory distance of approximately 0.34 m. Droplet D3 moved downward in both the radial and axial directions. Droplet D3 moved in a straight line up to a trajectory distance of about 0.335 m, and then the gravity effect was greater than the viscous effect until it reached the sedimentation velocity.

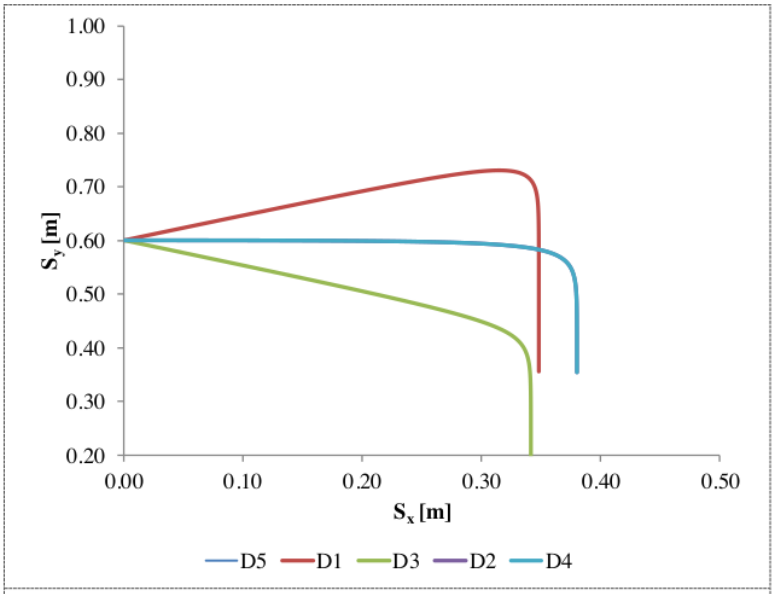

Figure 4. The intersection point of droplet collision between droplet D1 with droplet D5, and between droplet D1 with droplet D2 or D4

There are two possible collisions between droplet D1 and droplet D5, as well as between droplet D1 and droplet D2 or droplet D4. If the nozzle rotated at a certain rotational speed, a collision could occur. Figure 3 shows how all droplets move along their path when the nozzle does not turn. Droplet D1 may collide with droplets D2, D4, or D5 at the intersection point A when reaching the sedimentation velocity (Figure 4).

When one droplet collides with another, the gravity effect exceeds the viscous and causes the droplet to fall. The collision possibility between the droplets will have occurred when the droplets' trajectories intersect, as shown in Figure 4. In practice, the collision occurred only when the nozzle rotated at a specific rotational speed. A falling droplet may collide with a straight droplet moving faster. The time required by the nozzle to rotate a cycle was the difference in the travel times of two droplets to collide. When the droplets collide, the maximum rotational speed of the nozzle (or so-called critical rotational speed) can thus be calculated. Collisions could be avoided by rotating a nozzle at a slower rotational speed.

Theoretically, a collision between the droplets could be calculated based on the droplet's trajectory shown in Figure 4, point A. At point A, droplet D1 collided with droplet D5 with different travel times. Droplet D1 can then be hit by droplets D2 or D4. Droplet D5 traveled faster than droplet D1 to get to point A. The difference in travel time between droplets D1 and D5 to reach point A was the duration of the nozzle's rotational speed in a cycle of rotation. As a result, the critical nozzle rotation speed has been determined. Similarly, the time difference between droplets D2 or D4 and droplet D1 could be considered. To perform faster calculations and to simulate the droplet's trajectory over time, a spreadsheet was created. Each estimate would include velocity, viscosity, deceleration, and droplet path along the X, Y, and Z axes.

A spreadsheet calculation revealed a collision between droplets D1 and D5 at point A with coordinates of (0.348 m, 0.583 m). When droplet D5 moved for 0.086s and droplet D1 moved for 0.440 seconds, they collided. As a result of Equation (8), the maximum rotational speed required to cause the collision was 170 rpm.

$$n_{nozzle} = \frac{1\,cycle}{0.440s - 0.086s} \times \frac{60s}{\text{min}} = 170\ rpm \tag{8}$$

The collision between droplets at point A may move to a lower Y-axis as it is further examined in accordance with the illustration in Figure 6, specifically between droplet D1 and another below droplet D5. In that scenario, we suppose that droplet D1 and the new droplet D6 may collide. Droplet D6 had a starting point set at an angle qy of 67.5° and was located between droplets D5 and D3. A collision that could happen at a coordinate of (0.348 m; 0.371 m), or at the direction of the Y-axis opposite the previous Y-axis, was determined by the spreadsheet computation. Droplet D6 drifted for 0.246 seconds and droplet D1 drifted for 0.890 seconds before colliding. If the nozzle's rotating speed was 93 rpm as determined by Equation (9), the expected collision happened with a difference in travel time of approximately 0.644 seconds. As opposed to Equation (8), the droplets D1 and D6 collided at a slower rotating speed.

$$n_{nozzle} = \frac{1\,cycle}{0.890s - 0.246s} \times \frac{60s}{\text{min}} = 93\ rpm \tag{9}$$

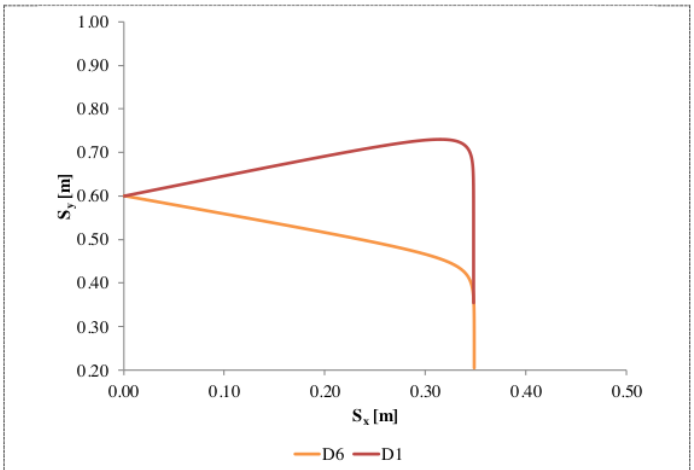

Figure 5. The collision simulation of droplet D1 by droplet D6 in the radial/horizontal direction (Z-axis) and axial/vertical direction (Y-axis)

Other collisions were possible between droplets D4 and D3 (defined as droplet D9) and D1, as well as a new pair of droplets D2 and D3 (defined as droplet D10) and D1. The droplets D9 and D10 are depicted in Figure 6.

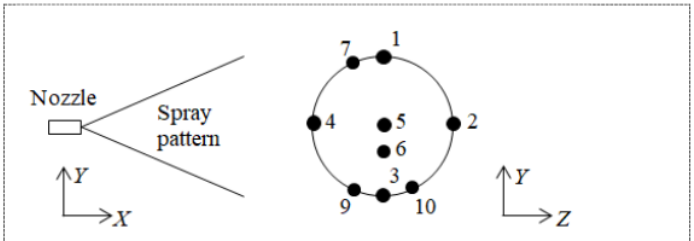

Figure 6. The location of droplets D6, D9, and D10 in the cross-section of the nozzle hole

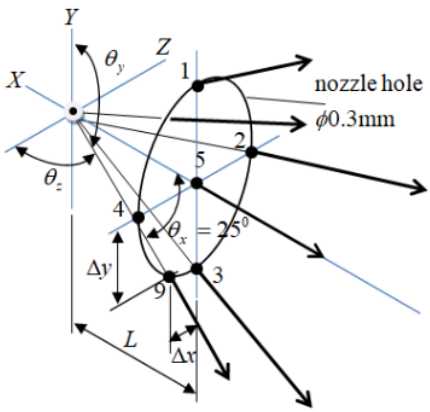

Figure 7. Mapping the initial location of droplet D9 in cross-section of the nozzle hole

Before calculating the trajectory of droplet D9 or droplet D10, the two droplets' initial locations must first be defined. Droplet D9's initial coordinate point at the nozzle hole was $\theta_x = 25°$, $\theta_y = 67.21°$, and $\theta_z = 78.58°$, whereas droplet D10's initial coordinate point was $\theta_x = 25°$, $\theta_y = 66.55°$, and $\theta_z = 80.30°$. Figure 7 depicts the isometrically described starting point of droplet D9 in the nozzle hole. The following describes the droplet D9 starting point calculation.

The distance L is the starting distance of the water spray: $L = \dfrac{0.15\ mm}{\tan 25^o} = 0.322\ mm$

Angle $\theta_z = 90^o - \dfrac{\Delta x}{L} = 90^o - \dfrac{0.065\ mm}{0.322\ mm} = 78.58^o$

$\Delta x^2 + \Delta y^2 = 0.3^2$

$\Delta y = \sqrt{0.3^2 - \Delta x^2} = 0.135\ mm$

Angle $\theta_y = 90^o - \tan^{-1}\dfrac{\Delta y}{L} = 90^o - \tan^{-1}\dfrac{0.135\ mm}{0.322\ mm} = 67.21^o$

After determining the initial coordinate point of droplet D9, the trajectory calculation produced the farthest radial distance of 0.348 m, which corresponds to the radial distance of droplet D1. The droplet D1 collided with droplet D9 at coordinate point (0.348 m; 0.360 m). Droplet D1 took 0.914 seconds to reach the collision point, while droplet D9 took 0.267 seconds to collide with droplet D1. The orbital circumference was determined by the orbital distance of droplet D9's return to the origin point. The circumference was measured as follows:

$$\text{Orbital circumference, } K_o = \pi\left(34.8\ cm\right) = 218.7\ cm$$

Droplet D9's required distance to collide with droplet D1 was not at a rotational speed or orbital circumference. If the nozzle rotates on the Y-axis toward the Z-axis, the distance was greater than a cycle.

$$K_o + L\sin\theta_x = 218.7\ cm + 34.8\sin 25^o = 233.4\ cm$$

Thus, as calculated in Equation (10), the magnitude of the critical rotational speed that caused a collision between droplets D1 and D9 was 99 rpm.

$$n_{nozzle} = \frac{\left(\frac{233.4}{218.7}\right) cycle}{0.914s - 0.267s} \times \frac{60s}{\min} = 99\ rpm \quad (10)$$

The following possible collision was between droplets D1 and D10. The droplet trajectory calculation yielded the farthest radial distance of 0.348 m, which equates to the radial distance of droplet D1. Droplet D1 may collide with Droplet D10 at the coordinates (0.348 m; 0.319 m). Droplet D1 needed 1.001 seconds to reach the collision point, and droplet D10 needed 0.346 seconds to collide with droplet D1. If droplet D1 collided with droplet D9 after droplet D9 rotated more than a cycle, droplet D10 needed a rotational speed less than a period and an orbital distance of 203.9 cm.

$$K_o - L\sin\theta_x = 218.7\ cm - 34.8\sin 25^o = 203.9\ cm$$

The magnitude of the critical rotational speed of droplet D1, collided by droplet D10, was 85.4 rpm as calculated by Equation (11).

$$n_{nozzle} = \frac{\left(\frac{203.9}{218.7}\right) cycle}{1.001s - 0.346s} \times \frac{60s}{\min} = 85.4\ rpm \quad (11)$$

A collision between two droplets was also possible between droplets D7 and D10. When the nozzle rotation speed has not reached a cycle, a collision between the two droplets may occur—this collision prediction is calculated at various positions of droplets D7 and D10. It predicted different nozzle rotation speeds with different starting point configurations. The collision prediction results of the two droplets at various initial coordinate points are shown in Table 1.

Table 1. Prediction of the collision between droplet D7 and droplet D10 at certain coordinates

The initial coordinate of droplet D7			The initial coordinate of droplet D10			Collision coordinate	t(D7) (s)	t(D10) (s)	Crit. rotational speed (rpm)
θ_x	θ_y	θ_z	θ_x	θ_y	θ_z				
25	70.83	72.72	25	72.41	71.12	0.363;0.399	0.754	0.252	111.5
25	66.27	81.16	25	68.01	76.88	0.352;0.372	0.872	0.251	90.1
25	65.05	88.22	25	66.55	80.30	0.348;0.319	1.000	0.346	85.6

The lowest critical rotational speed was 85.6 rpm. This rotational speed results in droplet D7 being closer to droplet D1 and droplet D10 being closer to droplet D3. However, the lowest critical rotational speed was not lower than the collision described above between droplets D1 and D10.

According to the calculated results, the obtained rotation speed from the possibility of collision between droplets D1 and D10 was the collision with the longest time difference. The rotational speed of 85.4 rpm was the lowest critical rotation speed possible in flashing with a rotating nozzle. The calculations performed and described above were performed under the assumption of constant water droplet size. While drifting in a vacuum chamber, the droplet size decreases due to evaporation. With a smaller droplet size, the collision may occur over a longer time interval, causing a nozzle to rotate slower than predicted by the above calculations.

The same calculations could be used to predict the effect of droplet size on evaporation. Assume that the size of the water droplet has been reduced to 80 microns. The lowest obtained nozzle rotation speed in the previous collision calculation between droplets D1 and D10 was 85.4 rpm. A collision between droplets D10 and D1 with diameters of 80 microns could occur at a coordinate point of (0.122 m; 0.539 m). Droplet D1 required 0.746 seconds of drifting time to reach the location, while droplet D10 required 0.064 seconds. As a result, if the nozzle rotates once per cycle, the critical rotational speed is 82 rpm, as shown in Equation (12).

$$n_{nozzle} = \frac{1\,cycle}{0.746s - 0.064s} \times \frac{60s}{\min} = 82\,rpm \quad (12)$$

As calculated in Equation (13), the critical rotational speed of the nozzle was 80 rpm if the droplet size was reduced to 40 μm.

$$n_{nozzle} = \frac{1\,cycle}{0.710s - 0.014s} \times \frac{60s}{\min} = 80\,rpm \quad (13)$$

The above calculations provided a quantitative representation of the effect of decreasing droplet size versus the nozzle's critical rotational speed. At lower rotational speeds, the smaller the droplet size, the greater the collision tendency. As a result, the distribution of water droplets in the flashing process by a rotating nozzle, accompanied by water droplet evaporation, was preferably performed below the critical rotational speed.

4. Conclusion

The critical rotational speed of the rotating nozzle can be predicted by calculating the kinematics of drifting water droplets within the flashing chamber. A smaller droplet size results in a slower rotational speed than a larger droplet size. For a water droplet diameter of 153.5 μm, the lowest nozzle rotational speed predicted is 85.4 rpm. A droplet with a diameter of 80 μm produces 82 rpm of nozzle rotational speed, while a droplet with a diameter of 40 μm produces 80 rpm of nozzle rotational speed. Evaporation may reduce the size of the water droplets during the flashing process. To avoid droplet collision and increase evaporation rate, finer water droplets require a lower nozzle rotational speed.

5. References

[1] Kitamura Y, Morimitsu H and Takahashi T 1986. Critical superheat for flashing of superheated liquid jets *Ind. and Eng. Chem. Fund.* **25** 206-11
[2] Miyatake O, Tomimura T, Ide Y and Fujii T 1981 An experimental study of spray flash evaporation *Desalination* **36** 113-128
[3] Mutair S and Ikegami Y 2008 Study and enhancement of flash evaporation desalination utilizing the ocean thermocline and discharged heat *Int. J. of Elec. and Comp. Eng.* **2** 1385-92
[4] Muthunayagam A, Ramamurthi K and Paden J 2005 Low-temperature flash vaporization for desalination *Desalination* **180** 25-32
[5] El-Fiqi A K, Ali N, El-Dessouky H, Fath H and El-Hefni M 2007 Flash evaporation in a superheated water liquid jet *Desalination* **206** 311-21
[6] Goto S, Yamamoto Y, Sugi T, Yasunaga T, Ikegami Y and Nakamura M 2008 A simulation model of spray flash desalination system *IFAC Proc.* **41** 15909-14
[7] Ikegami Y, Sasaki H, Gouda T and Uehara H 2006 Experimental study on a spray flash desalination (influence of the direction of injection) *Desalination* **194** 81-89
[8] Karami R, Ashgriz N and Tran H 2010 The effect of flashing on characteristics of sprays of splash-plate nozzles *ILASS Americas*
[9] El-Zahaby A, Kabeel A, Bakery A, Agouz E and Hawam O 2009 Enhancement of solar desalination still productivity using flash evaporation *Thirteenth Int. Water Tech. Conf.* 1443-59
[10] Chen Q, Li Y and Chua K 2018 Experimental and mathematical study of the spray flash evaporation phenomena *Appl. Therm. Eng.* **130** 598-610

The theoretical approach of how to predict the critical rotational speed of the rotating nozzle in flashing purification to increase the evaporation rate

ORIGINALITY REPORT

8%	8%	9%	5%
SIMILARITY INDEX	INTERNET SOURCES	PUBLICATIONS	STUDENT PAPERS

MATCH ALL SOURCES (ONLY SELECTED SOURCE PRINTED)

8%

★ www.researchgate.net

Internet Source

Exclude quotes	On	Exclude matches	< 1%
Exclude bibliography	On		